

Magnetomicelles: Composite Nanostructures from Magnetic Nanoparticles and Cross-Linked Amphiphilic Block Copolymers

Byeong-Su Kim,[†] Jiao-Ming Qiu,[‡] Jian-Ping Wang,[‡] and T. Andrew Taton^{*†}

*Department of Chemistry and Department of Electrical and Computer Engineering,
University of Minnesota, 207 Pleasant Street SE, Minneapolis, Minnesota 55455*

Received July 19, 2005; Revised Manuscript Received August 30, 2005

ABSTRACT

We report the synthesis, characterization, and covalent surface chemistry of “magnetomicelles”, cross-linked, amphiphilic block-copolymer micelles that encapsulate superparamagnetic iron oxide nanoparticles. Because these composite nanostructures assemble spontaneously from solution by simultaneous desolvation of nanoparticle and amphiphilic poly(styrene₂₅₀-*block*-acrylic acid₁₃) components, explicit surface functionalization of the particles is not required, and the encapsulation method was applied to different magnetic nanoparticle sizes and compositions. TEM images of the magnetomicelles illustrated that the number of encapsulated particles could be dictated rationally by synthetic conditions. The magnetic properties of the particles were characterized by SQUID magnetometry and followed the general Langevin magnetic model for superparamagnetic materials. The micellar shells of these particles were functionalized using covalent chemistry that would not ordinarily be possible on the magnetic particle surface. As a result, this noncovalent approach provides a new route to technological applications of hydrophobic magnetic nanomaterials that lack appropriate conjugate surface chemistry.

Magnetic nanoparticles are playing increasingly important roles in biotechnology and biomedicine.¹ For example, they have been used as carriers for magnetic drug targeting,² as tags for biomolecular sensors,^{3,4} and in biomolecule separation and purification,^{5–7} *in vivo* imaging,^{8–10} and magneto-thermal therapy.^{11,12} As these and other applications become more sophisticated, precise control over the stability and surface functionality of magnetic nanostructures is critical. Surface coatings for magnetic nanoparticles have been developed that prevent aggregation, enhance compatibility of nanoparticles with solid matrices or improve their stability in suspension, and provide chemical handles for further conjugation. This has been achieved by covalent attachment of small-molecule ligands,^{6,13} by adsorption of passivating polymers,^{14–16} or by ligand-initiated growth of silica^{17–21} or polymer shells^{22,23} around the particles. An alternative approach to stabilizing and functionalizing magnetic nanoparticles in aqueous solution involves the spontaneous self-assembly of magnetic core, amphiphile block-copolymer shell nanostructures. For example, Euliss et al. demonstrated recently that amphiphilic block copolypeptides can be assembled around clusters of γ -Fe₂O₃ nanoparticles to form

water-soluble, composite nanostructures.²⁴ Herein, we report that amphiphilic poly(styrene₂₅₀-*block*-acrylic acid₁₃) (PS₂₅₀-*b*-PAA₁₃) copolyolefin similarly coassembles with magnetic nanoparticles to enclose the particles within copolymer micelles (Scheme 1).

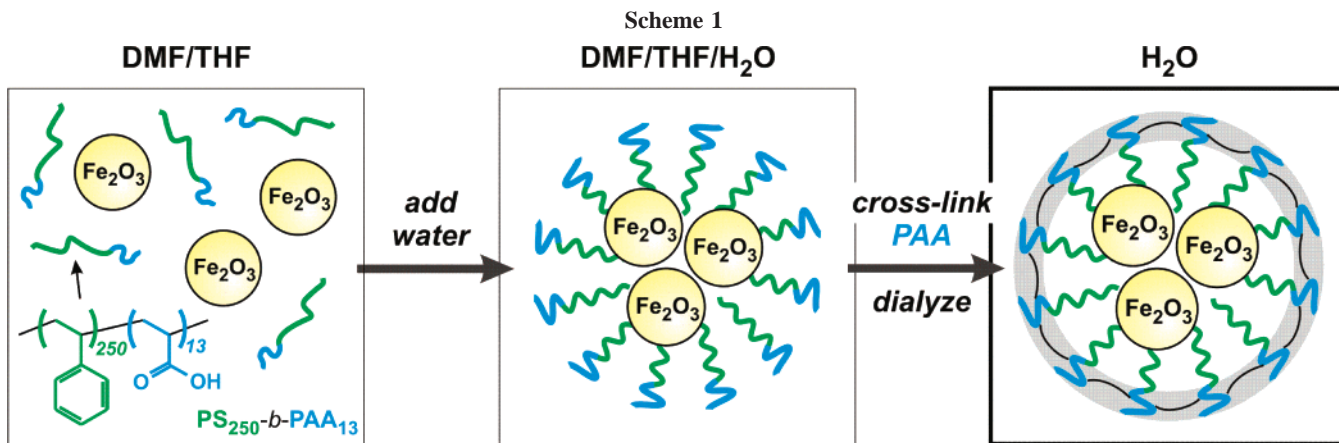
Furthermore, we demonstrate that the surrounding polymer can be cross-linked to fix the nanostructures topologically and these structures are stable to further synthetic transformations of surface functional groups. Because shell assembly does not require covalent interaction between the copolymer shell and the nanoparticle core, we argue that this method is particularly well suited to protecting and functionalizing materials such as γ -Fe₂O₃ for which strongly binding surface ligands are not readily available.

To synthesize magnetic-core copolymer-shell nanostructures, we used an approach developed previously to encapsulate gold nanoparticles²⁵ and carbon nanotubes²⁶ within block-copolymer micelles. Initially, oleic acid-stabilized, monodisperse γ -Fe₂O₃ nanoparticles were synthesized by thermal decomposition of Fe(CO)₅ in hydrocarbon solvent, followed by further oxidation using (CH₃)₃NO, as previously reported.²⁷ This synthesis yielded relatively monodisperse and crystalline γ -Fe₂O₃ nanoparticles, which were characterized by transmission electron microscopy (TEM) (Figure 1a), selected-area electron diffraction (SAED), and X-ray diffraction (XRD).²⁸ The amphiphilic block copolymer, PS₂₅₀-

* To whom correspondence should be addressed. E-mail: taton@chem.umn.edu.

[†] Department of Chemistry.

[‡] Department of Electrical and Computer Engineering.



$b\text{-PAA}_{13}$ ($M_n = 27\,000$ g/mol; PDI = 1.15),²⁹ was synthesized via atom-transfer radical polymerization following a published protocol.²⁵ The block copolymer was first dissolved in *N,N*-dimethylformamide (DMF), a good solvent for both the hydrophobic (PS) and hydrophilic (PAA) blocks. A solution of nanoparticles in tetrahydrofuran (THF) was then combined with the DMF solution of polymer in a defined ratio, and water was added gradually to this mixture to desolvate both the particles and the hydrophobic polymer block simultaneously. In the absence of block copolymer, $\gamma\text{-Fe}_2\text{O}_3$ nanoparticles flocculated from suspension as water was added. However, in the presence of $\text{PS}_{250}\text{-}b\text{-PAA}_{13}$, water served as a selective nonsolvent for both the hydrophobic PS block and hydrophobic nanoparticles and induced the formation of micelles around the nanoparticles. Encapsulation of oleic acid-capped particles was successful, but the quality of the micelles (as determined by TEM images at this stage) was improved qualitatively if the oleic acid was first exchanged for 11,11-bis-hydroxymethyl undecosane (diol), a better surface ligand for $\gamma\text{-Fe}_2\text{O}_3$.^{6,13} The PAA block of the assembled copolymer was fixed permanently with 2,2'-(ethylenedioxy)bis(ethylamine) cross-linker and *N*-ethyl-*N'*-(3-dimethylaminopropyl)carbodiimide methiodide (EDC) activator.^{25,26,30} The amounts of cross-linker and activator used were calculated based on the number of acrylic acid monomer units present in the original polymer concentration; 0.50 equiv activator and 0.25 equiv diamine cross-linker were sufficient to yield magnetomicelles that could be stored stably for months but still possessed free surface carboxylates for

further manipulation. Excess reagents were removed by dialysis (Spectra/Por 4, MWCO = 12–14 K) of the suspension against Nanopure water (18 M Ω) after cross-linking, followed by successive cycles of filtration and centrifugation. This procedure afforded magnetomicelles in which particles were confined exclusively within micelle cores (Figure 1b).

The average number of encapsulated particles per micelle (N_{ave}) could be controlled by varying the relative starting concentrations of nanoparticles and polymer (Figure 2). Increasing numbers of nanoparticles were incorporated into each micelle with increasing particle concentration, and the distribution of particles among micelles in each sample was roughly Gaussian. This behavior is consistent with the nanoparticles acting as simple hydrophobic solubilizes that localize to micelle cores in aqueous solution.^{31,32} As is the case for small-molecule solute swelling of polymer micelles,³³ the size of magnetomicelles scaled with the number of encapsulated nanoparticle solubilizes (Figure 2g). We observed similar behavior previously in the encapsulation of small ($d < 10$ nm) metal nanoparticles.³⁴ Surface templating in that study allowed gold particles with $d > 10$ nm to be singly encapsulated in $\text{PS-}b\text{-PAA}$, but we were unable to synthesize magnetomicelles containing exclusively one $\gamma\text{-Fe}_2\text{O}_3$ particle in this work, even at low starting nanoparticle concentrations.

In samples in which a substantial fraction of micelles contain one or few particles, the thick polymer shell had the expected effect of limiting magnetic coupling between particles. To characterize this effect, we characterized magnetomicelle samples with different N_{ave} by superconducting quantum interference device (SQUID) magnetometry (Figure 3). Measured $M\text{-}H$ curves showed no hysteresis, indicating that the $\gamma\text{-Fe}_2\text{O}_3$ nanoparticle assemblies were superparamagnetic. All data could be fit to the Langevin function for paramagnetic particles.³⁵ Relative susceptibilities, κ , (measured by the slope at the $M\text{-}H$ curve origin) for samples of magnetomicelles with $N_{\text{ave}} > 4$ were identical to those measured for diol-capped $\gamma\text{-Fe}_2\text{O}_3$ nanoparticle starting material that had been concentrated and dried onto a substrate. This indicated efficient magnetic coupling between particles in these magnetomicelles. However, $M\text{-}H$ curves

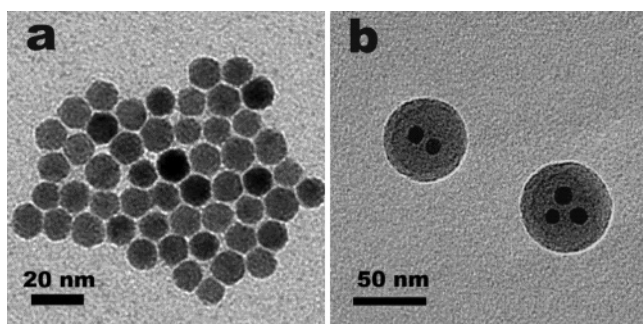


Figure 1. TEM images of 10.9 nm $\gamma\text{-Fe}_2\text{O}_3$ nanoparticles (a) before and (b) after encapsulation within $\text{PS}_{250}\text{-}b\text{-PAA}_{13}$ micelles.

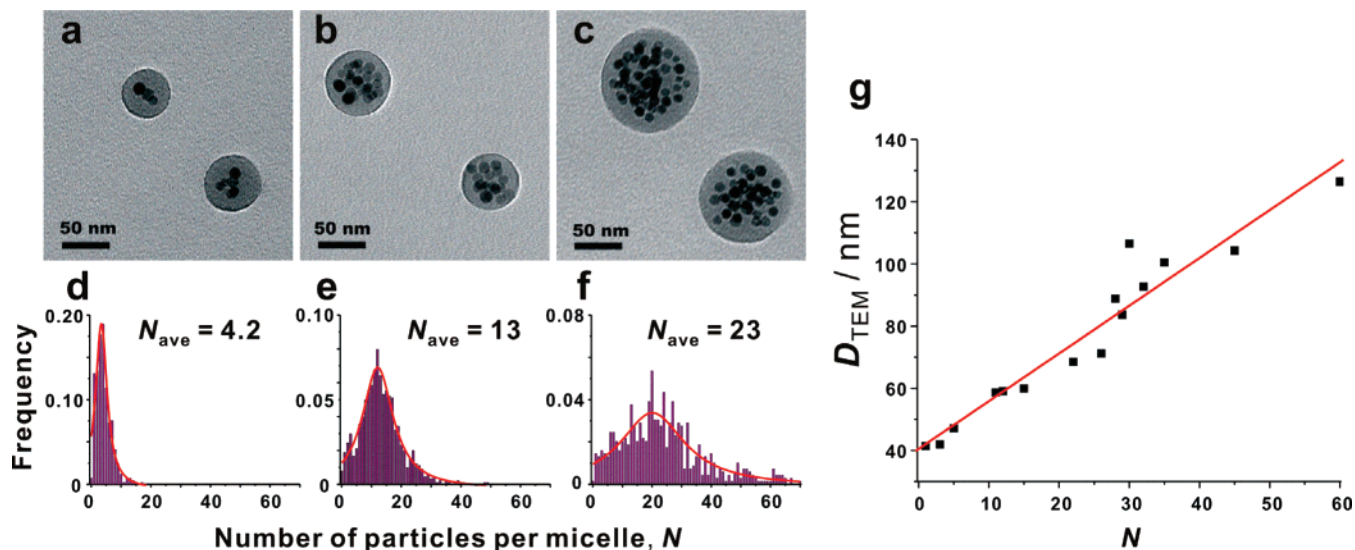


Figure 2. (a–c) TEM images of 10.9 nm γ -Fe₂O₃ nanoparticles encapsulated within PS₂₅₀-*b*-PAA₁₃ micelles, synthesized with $[\gamma$ -Fe₂O₃]_{initial} = (a) 0.10 mg/mL, (b) 0.30 mg/mL, and (c) 0.50 mg/mL at fixed polymer concentration ($[\text{PS}_{250}\text{-}b\text{-PAA}_{13}]_{\text{initial}} = 0.10$ mg/mL) in 50:50 DMF/THF. (d–f) Corresponding histograms of the number of counted particles (N) encapsulated within each micelle for samples shown in a–c, averaged over 500 magnetomicelles. (g) Average diameter of selected magnetomicelles obtained from TEM (D_{TEM}) as a function of N . Because deposition and drying on the TEM grid commonly affect the observed diameter of micelles,²⁸ D_{TEM} values do not necessarily represent the actual diameters of the magnetomicelles in suspension.

for samples with $N_{ave} < 4$ showed lower relative susceptibility, which we attribute to less effective coupling caused by increased first-neighbor distance.³⁶

Magnetomicelles containing $N_{ave} > 13$ in aqueous suspension migrated rapidly toward a strong bar magnet (NdFeB magnet, 0.14 T at 1 cm). As is also typical for microscale magnetic beads, these composite nanoparticles could be attracted to the bottom of an Eppendorf tube, the aqueous supernatant removed, and the particles resuspended without significant material loss or aggregation. Drying the material under an applied magnetic field did result in field-aligned chains of magnetomicelles (Supporting Information Figure S7²⁸), as has been described for larger superparamagnetic nanoparticles.³⁷ However, no such structures were observed in the TEM images of the samples dried onto TEM grids in the absence of an applied field. We expect that the dispersibility of these magnetic nanostructures will be advantageous

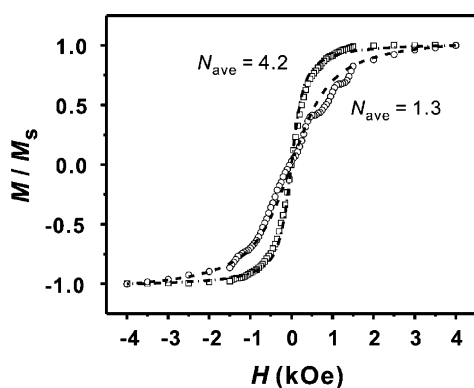


Figure 3. SQUID $M-H$ curve measurements on magnetomicelles with $N_{ave} = 4.2$ (\square) and $N_{ave} = 1.3$ (\circ) 10.9 nm γ -Fe₂O₃ nanoparticles per micelle. Fits to the Langevin paramagnetic model (eq 1) are also displayed for each dataset (dashed line).

for their use in biotechnological applications that are commonly performed with magnetic microbeads, such as biomolecule and cell separation.

A primary goal of this research was to prepare magnetomicelles that could be functionalized controllably with organic or biological molecules. Previous work has shown that amine-containing molecules can be attached to the shells of PAA-block micelles by EDC-mediated coupling.^{39,40} To characterize the coupling of amines to the surface of PAA-shell magnetomicelles, particle suspensions were exposed to EDC and *N*-hydroxylsulfosuccinimide sodium salt, followed by controlled equivalents of the fluorescent model compound α -amino- γ -[5(6)carboxamidofluorescein]-pentaethyleneglycol (NH₂-EG₅-FAM).²⁸ The reaction product was then dialyzed extensively against water, followed by centrifugation and redispersion, to remove unreacted fluorescent species. The extent of functionalization could be controlled by the stoichiometry of the amine reactant (Figure 4), and at least 600 molecules of NH₂-EG₅-FAM were bound to the surface of each magnetomicelle when saturated.²⁸ TEM analysis of the resulting product demonstrated that magnetomicelles maintained their structural integrity after functionalization.

We have evaluated this noncovalent encapsulation method successfully for various iron oxide nanoparticles, including different sizes of γ -Fe₂O₃²⁷ ($d = 3.8, 6.3, 10.4$ nm) as well as Fe₃O₄⁴¹ ($d = 5.6$ nm), within PS₂₅₀-*b*-PAA₁₃ (Figure 5). In all of these cases, the hydrophobic micelle cores physically isolated the encapsulated particles from their aqueous environment. To test the permeability of the polymer shell, magnetomicelles containing 10.9 nm diameter γ -Fe₂O₃ were resuspended in aqueous HCl (pH 2), a known etchant for iron oxide.^{42,43} TEM analysis showed that the encapsulated particles were not affected by this treatment. By contrast, surface-bound polymers were shown previously not to shield

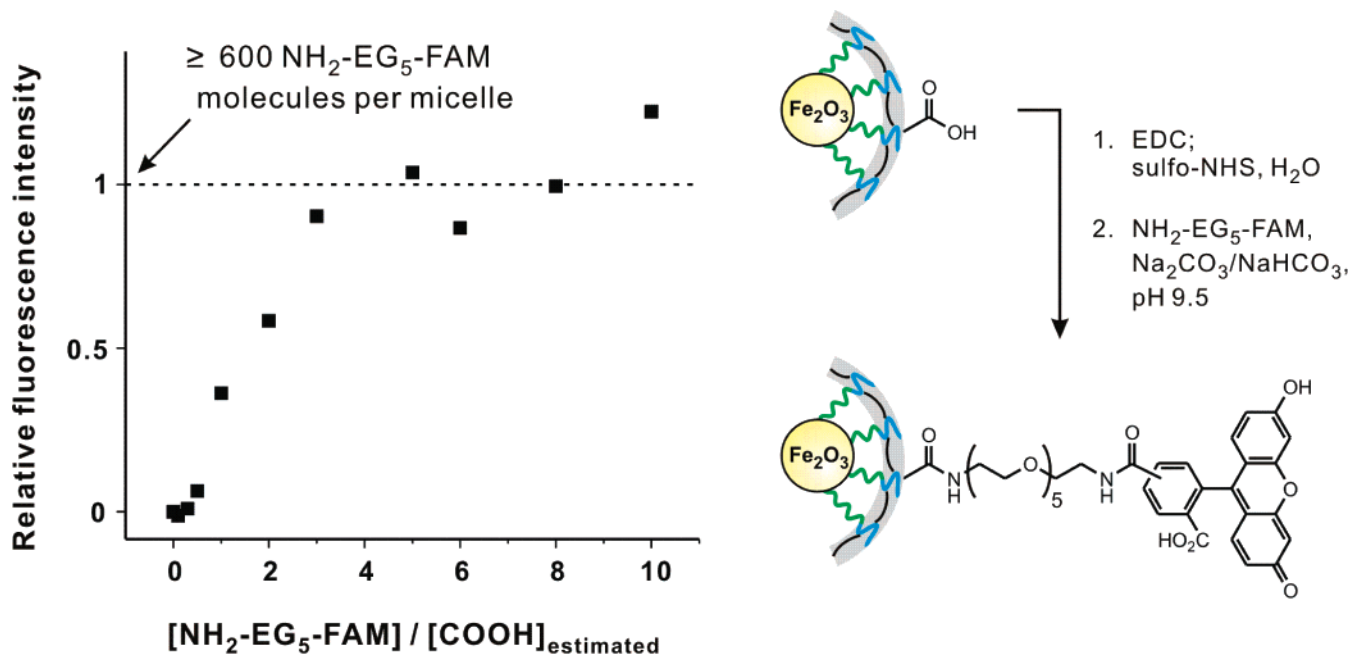


Figure 4. Fluorescence intensity of magnetomicelles isolated from reactions with varying equivalents of α -amino- γ -[5(6)-carboxamido-fluorescein]-pentaethyleneglycol ($\text{NH}_2\text{-EG}_5\text{-FAM}$). Equivalents were calculated from the estimated number of available carboxylic acid groups in the micelle sample (after 50% cross-linking of the PAA shells). Fluorescence intensities are corrected for background scattering, determined from control mixtures of $\text{NH}_2\text{-EG}_5\text{-FAM}$ and nonactivated magnetomicelles. Estimating a micelle concentration (0.82 pM) based on the initial polymer concentration and the average, TEM-measured micelle diameter (54 nm), the average maximum fluorescence intensity corresponds to 500 pM surface-bound $\text{NH}_2\text{-EG}_5\text{-FAM}$, or at least 600 fluorophores per nanostructure.²⁸ At this functionalization density, fluorophores are closer to each other than the Förster distance for radiationless energy transfer (self-quenching).³⁸ As a result, this number represents a lower limit to the number of $\text{NH}_2\text{-EG}_5\text{-FAM}$ molecules bound to each magnetomicelle.

magnetic particles from similar etching conditions.^{22,42,43} Magnetomicelle suspensions were stable to a variety of biological buffer systems over a wide pH range (pH 2–11). These results demonstrate that, as noted previously for

micelle-encapsulated gold nanoparticles,²⁵ the copolymer shell provides a physical barrier that isolates and protects the enclosed magnetic nanoparticles. As expected, however, adding large amounts (>80 vol %) of organic cosolvent, such as DMF or THF, solvated the core PS block and flocculated the particles.

In summary, we have demonstrated the encapsulation of magnetic nanoparticles within amphiphilic block-copolymer micelles as a route toward composite, core/shell magnetic nanostructures. The magnetic properties of these structures can be controlled by varying the relative concentrations of the magnetic nanoparticles and encapsulating polymer. We have also established that the hydrophilic shell can be functionalized chemically without diminishing the stability or structure of the micelle coat. Following this research and our similar work with gold nanoparticles^{25,34,44} and single-walled carbon nanotubes,²⁶ we are currently investigating the approach as a means of protecting and functionalizing inorganic nanostructures made from other materials and in other shapes. Overall, we predict that these self-assembled, water-soluble nanostructures will be useful in biotechnological protocols that other micro- and nanomaterials (e.g., carboxylated magnetic microbeads) do not survive.

Acknowledgment. This work was supported by the NIH (1 R21 EB003809-01).

Supporting Information Available: Detailed procedures for the preparation of magnetomicelle and characterization data, SAED, FT-IR, and additional TEM images. Details of

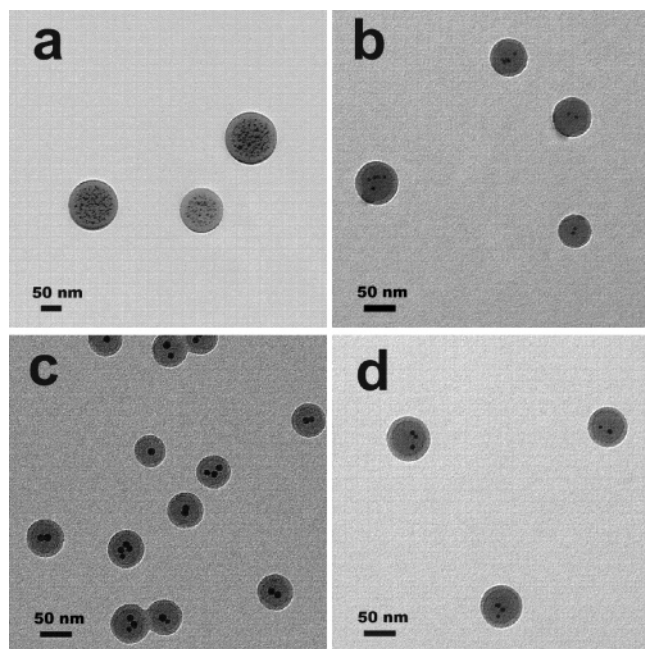


Figure 5. (a–d) TEM images of different hydrophobic nanoparticles encapsulated within $\text{PS}_{250}\text{-}b\text{-PAA}_{13}$ micelles. (a) 3.8 nm $\gamma\text{-Fe}_2\text{O}_3$, (b) 6.4 nm $\gamma\text{-Fe}_2\text{O}_3$, (c) 10.4 nm $\gamma\text{-Fe}_2\text{O}_3$, and (d) 5.6 nm Fe_3O_4 .

Langevin fitting process and determination of surface functionalization of magnetomicelles. This material is available free of charge via the Internet at <http://pubs.acs.org>.

References

- (1) Pankhurst, Q. A.; Connolly, J.; Jones, S. K.; Dobson, J. J. *Phys. D: Appl. Phys.* **2003**, *36*, R167–R181.
- (2) Alexiou, C.; Jurgons, R.; Schmid, R. J.; Bergemann, C.; Henke, J.; Erhardt, W.; Huenges, E.; Parak, F. *J. Drug Targeting* **2003**, *11*, 139–149.
- (3) Perez, J. M.; Simeone, F. J.; Saeki, Y.; Josephson, L.; Weissleder, R. *J. Am. Chem. Soc.* **2003**, *125*, 10192–10193.
- (4) Graham, D. L.; Ferreira, H. A.; Freitas, P. P. *Trends Biotechnol.* **2004**, *22*, 455–462.
- (5) Bucak, S.; Jones, D. A.; Laibinis, P. E.; Hatton, T. A. *Biotechnol. Prog.* **2003**, *19*, 477–484.
- (6) Xu, C.; Xu, K.; Gu, H.; Zheng, R.; Liu, H.; Zhang, X.; Guo, Z.; Xu, B. *J. Am. Chem. Soc.* **2004**, *126*, 9938–9939.
- (7) Gu, H.; Ho, P.-L.; Tsang, K. W. T.; Wang, L.; Xu, B. *J. Am. Chem. Soc.* **2003**, *125*, 15702–15703.
- (8) Bulte, J. W. M.; Douglas, T.; Witwer, B.; Zhang, S.-C.; Strable, E.; Lewis, B. K.; Zywicke, H.; Miller, B.; van Gelderen, P.; Moskowitz, B. M.; Duncan, L. D.; Frank, J. A. *Nat. Biotechnol.* **2001**, *19*, 1141–1147.
- (9) Lewin, M.; Carlesso, N.; Tung, C.-H.; Tang, X.-W.; Cory, D.; Scadden, D. T.; Weissleder, R. *Nat. Biotechnol.* **2000**, *18*, 410–414.
- (10) Mornet, S.; Vasseur, S.; Grasset, F.; Duguet, E. *J. Mater. Chem.* **2004**, *14*, 2161–2175.
- (11) Hiergeist, R.; Andra, W.; Buske, N.; Hergt, R.; Hilger, I.; Richter, U.; Kaiser, W. *J. Magn. Magn. Mater.* **1999**, *201*, 420–422.
- (12) Jordan, A.; Scholz, R.; Wust, P.; Fahling, H.; Felix, R. *J. Magn. Magn. Mater.* **1999**, *201*, 413–419.
- (13) Boal, A. K.; Das, K.; Gray, M.; Rotello, V. M. *Chem. Mater.* **2002**, *14*, 2628–2636.
- (14) Pellegrino, T.; Manna, L.; Kudera, S.; Liedl, T.; Koktysh, D.; Rogach, A. L.; Keller, S.; Raedler, J.; Natile, G.; Parak, W. J. *Nano Lett.* **2004**, *4*, 703–707.
- (15) Xu, X. L.; Friedman, G.; Humfeld, K. D.; Majetich, S. A.; Asher, S. A. *Adv. Mater.* **2001**, *13*, 1681–1684.
- (16) Gomez-Lopera, S. A.; Plaza, R. C.; Delgado, A. V. *J. Colloid Interface Sci.* **2001**, *240*, 40–47.
- (17) Yi, D. K.; Selvan, S. T.; Lee, S. S.; Papaefthymiou, G. C.; Kundaliya, D.; Ying, J. Y. *J. Am. Chem. Soc.* **2005**, *127*, 4990–4991.
- (18) Wang, D.; He, J.; Rosenzweig, N.; Rosenzweig, Z. *Nano Lett.* **2004**, *4*, 409–413.
- (19) Lu, Y.; Yin, Y. D.; Mayers, B. T.; Xia, Y. N. *Nano Lett.* **2002**, *2*, 183–186.
- (20) Levy, L.; Sahoo, Y.; Kim, K. S.; Bergey, E. J.; Prasad, P. N. *Chem. Mater.* **2002**, *14*, 3715–3721.
- (21) Tartaj, P.; Serna, C. J. *J. Am. Chem. Soc.* **2003**, *125*, 15754–15755.
- (22) Wang, Y.; Teng, X. W.; Wang, J. S.; Yang, H. *Nano Lett.* **2003**, *3*, 789–793.
- (23) Vestal, C. R.; Zhang, Z. J. *J. Am. Chem. Soc.* **2002**, *124*, 14312–14313.
- (24) Euliss, L. E.; Grancharov, S. G.; O'Brien, S.; Deming, T. J.; Stucky, G. D.; Murray, C. B.; Held, G. A. *Nano Lett.* **2003**, *3*, 1489–1493.
- (25) Kang, Y.; Taton, T. A. *Angew. Chem., Int. Ed.* **2005**, *44*, 409–412.
- (26) Kang, Y.; Taton, T. A. *J. Am. Chem. Soc.* **2003**, *125*, 5650–5651.
- (27) Hyeon, T.; Lee, S. S.; Park, J.; Chung, Y.; Bin Na, H. *J. Am. Chem. Soc.* **2001**, *123*, 12798–12801.
- (28) See the Supporting Information for further details of synthesis and characterization.
- (29) Values derived from GPC and NMR analysis of precursor PS-*b*-PtBA polymer.
- (30) Huang, H. Y.; Remsen, E. E.; Kowalewski, T.; Wooley, K. L. *J. Am. Chem. Soc.* **1999**, *121*, 3805–3806.
- (31) Zhao, J. X.; Allen, C.; Eisenberg, A. *Macromolecules* **1997**, *30*, 7143–7150.
- (32) Xing, L.; Mattice, W. L. *Langmuir* **1998**, *14*, 4074–4080.
- (33) Nagarajan, R.; Ganesh, K. *J. Colloid Interface Sci.* **1996**, *184*, 489–499.
- (34) Kang, Y.; Taton, T. A. *Macromolecules* **2005**, *38*, 6115–6121.
- (35) Bean, C. P.; Livingston, J. D. *J. Appl. Phys.* **1959**, *30*, 120S–129S.
- (36) Russier, V.; Petit, C.; Pileni, M. P. *J. Appl. Phys.* **2003**, *93*, 10001–10010.
- (37) Butter, K.; Bomans, P. H. H.; Frederik, P. M.; Vroege, G. J.; Philipse, A. P. *Nat. Mater.* **2003**, *2*, 88–91.
- (38) Kowski, A. *Photochem. Photobiol.* **1983**, *38*, 487–508.
- (39) Pan, D.; Turner, J. L.; Wooley, K. L. *Chem. Commun.* **2003**, 2400–2401.
- (40) Becker, M. L.; Remsen, E. E.; Pan, D.; Wooley, K. L. *Bioconjugate Chem.* **2004**, *15*, 699–709.
- (41) Sun, S. H.; Zeng, H.; Robinson, D. B.; Raoux, S.; Rice, P. M.; Wang, S. X.; Li, G. X. *J. Am. Chem. Soc.* **2004**, *126*, 273–279.
- (42) Li, G. F.; Fan, J. D.; Jiang, R.; Gao, Y. *Chem. Mater.* **2004**, *16*, 1835–1837.
- (43) Matsuno, R.; Yamamoto, K.; Otsuka, H.; Takahara, A. *Macromolecules* **2004**, *37*, 2203–2209.
- (44) Ge, Z.; Kang, Y.; Taton, T. A.; Braun, P. V.; Cahill, D. G. *Nano Lett.* **2005**, *5*, 531–535.

NL0513939